URBAN HEAT ISLAND EFFECT ANALYSIS USING INTEGRATED GEOSPATIAL TECHNIQUES: A CASE STUDY ON KHULNA CITY, BANGLADESH

Conference Paper · March 2019

CITATIONS
13

READS
1,908

4 authors:

Kazi Saiful Islam
Khulna University
53 PUBLICATIONS **233** CITATIONS
SEE PROFILE

Md Didarul Islam
George Mason University
21 PUBLICATIONS **226** CITATIONS
SEE PROFILE

Torit Chakraborty
Khulna University
18 PUBLICATIONS **215** CITATIONS
SEE PROFILE

Md. Shaharier Alam
University of Florida
32 PUBLICATIONS **445** CITATIONS
SEE PROFILE

URBAN HEAT ISLAND EFFECT ANALYSIS USING INTEGRATED GEOSPATIAL TECHNIQUES: A CASE STUDY ON KHULNA CITY, BANGLADESH

[1] M.D. Islam [2]T. Chakraborty* [3]M.S .Alam,[4] K.S. Islam.

[1,2,3] *Urban And Rural Planning Discipline, Khulna University, Khulna-9208, Bangladesh*

[4] *Professor, Urban And Rural Planning Discipline, Khulna University, Khulna-9208, Bangladesh*

[*]Corresponding author email: ***toritchakraborty@gmail.com***

Abstract

In recent years, the world is facing a drastic climate change which affect specially in seasonal change and global temperature. Due to geographical setting, Bangladesh is one of the front-line of global climatic change which ultimately leads to its seasonal variation and duration. As the global temperature is increasing gradually, it's effect should be considered for making strategy to ensure smart and sustainable cities. So, in this study, we conducted research on Urban heat island effect analysis using integrated GIS and remote sensing to assess the land surface temperature variation with spatial distribution of land cover. Khulna city is selected to conduct the research to assess the urban heat island effect in relation to the land cover change over the years. The Landsat imagery from 2001, 2011 and 2018-years are used in this research. The support vector machine algorithm is used to classify land cover for the 3 years and the accuracy of the classification is evaluated by the cohen kappa score. Spatial co-relation between land cover and land surface temperature is discussed and analyzed here to identify the heat island effect based on the change of land cover types over the years. The result shows that there is a co-relation existing between urban land surface temperature and land cover change. This finding can be used for formulating effective planning strategies to minimize the urban heat island effect. So, this research presents the overall scenario of the urban heat island effect of the Khulna city with respect to land cover change and provide a guideline to take effective and efficient planning initiatives towards the climate change event.

Keywords: Urban heat island effect, Land cover, Land Surface temperature, Geographic Information system, Remote sensing

1.Introduction

Climate change and its effect on the environment and habitat is a global issue which is one of the biggest concern in the 21st century. Urban heat island effect is one of them which refers to the higher temperature intensity in the urban area due to its urban settings and high density built-up area than the rural areas. Actually the urban setting is one of the main reason of the temperature variation because of the surface structure like high density built-up area, haphazard physical infrastructures etc. which absorb and reflect more temperature than other land cover types. Land surface temperature is very important and effective parameter to take different types of decision regarding environmental issues and also used in various environmental model, urban planning and in so many fields (Becker ,1990**).** The uncontrolled population growth is one of the major cause of urban land cover change (Coskun,2008**).** The increasing population is the driven factor of urbanization which influenced the conversion of land cover change that ultimately results the declination in water body, forest cover and agriculture land drastically which leads to the change in local climate specially in surface temperature as the urban land cover has strong capacity of absorption of solar radiation, evaporation rates, thermal storage of surface. So these micro-climatic impact in local level as increasing land surface temperature directs the global climate change in wider scale (Igun, 2018).

In recent years, the advancement of geospatial techniques make urban and environmental related analysis easier and effective and help to solve real world problem. So, in this research, Integrated GIS & RS techniques were used to analyze and visualize the land surface temperature in relation to land cover change over the years.

2.Methodology

2.1 Study area: Khulna city corporation area is selected for this study as Khulna city is the third metropolitan city of Bangladesh and most potential for growth due to several government policy in

recent years including Padma bridge. The KCC area is 45.65 km^2 with 31 wards and its maximum, minimum temperature is 35.5 ^{0} C & 12.5 ^{0} C (KCC, 2018)

2.2 Data collection & data processing: In this research, mainly satellite imagery were used to analyze LST, land cover classification & change detection. The Landsat TM for 2001 and 2011 and Landsat 8 TIRS/OLI for 2018 were collected from USGS earth explorer website with less than 10% cloud coverage.

Table.1-*Specification Landsat satellite images*

Satellite	Sensors	Acquisition date	Path/Row	Number of bands	Radiometric resolution	Spatial resolution (m
Landsat 5	TM	April 15,2001	138/44	7	8 bit	30
Landsat 5	TM	March 30,2011	138/44	7	8 bit	30
Landsat 8	OLI/TIRS	May 30,2018	138/44	11	16 bit	30

All the images were captured carefully in summer season to avoid sessional variation in thermal band. Both satellite image- Landsat TM & TIRS/OLI data is combined in a single composite band for further analysis using layer stacking tool in ERDAS IMAGINE software. The study area map is clipped from the three images by using the subset tool in ERDAS IMAGINE. Then atmospheric corrections operation was conducted using FLAASH module by ENVI 5.3 software on the three images to avoid atmospheric distortion. Some radiometric and spatial image enhancing techniques like histogram equalization, edge enhancement, contrast & brightness balance were used for better visualization and best suit for further analysis.

2.3 Data analysis

In this research, we mainly focused on two analysis, land cover classification with change detection & land surface temperature calculation and finding relationship with land cover change.

Land Cover classification: As this research has the major focus on to find out the relationship between the land cover and LST, the Landsat imagery was classified into four categories namely built-up area, barren land, water body and vegetation. Built-up area was indicated as residential, commercial, industrial, settlements and physical infrastructures; barren land as open space, bare lands, bare soil; vegetation as crop fields, trees, grasslands; waterbody as river, pond etc. For land cover classification, supervised methods applied for classification. We mainly used three machine algorithms namely k-nearest neighbor, support vector machine (SVM) and maximum likelihood classifier in supervised method on training data. We also used parameter tuning of the algorithms to increase the classification capability and accuracy. As we used three machine learning algorithms to get highest accurate classified image, we also used combination of different parameters of algorithms to determine the best fitted parameters for individual algorithms. For this, we utilized Grid Search method of scikit-learn package of python programming language. Then those best fitted parameters of a particular algorithms used to train and classify satellite image.

Then we used different statistics including cohen kappa to assess and validate the accuracy of the model. The output map of the highest accurate model was used for the final analysis.

Retrieval of LST: Thermal band of Landsat TM and TIRS was used to retrieve land surface temperature (Sobrino et. al., 2004) of the study area. For Landsat 5 TM data, wavelength of band 6 (10.40-12.50μm) falls under thermal region. Wavelength of band 10 (10.60 - 11.19μm) and 11 (11.50 - 12.51μm) of Landsat 8 TIRS data falls under thermal region. But due to higher calibration uncertainty associated with band 11 (USGS, 2014), it is not recommended for LST retrieval. Instead, band 10 gain higher accuracy in terms of LST retrieval than band 11 (Jimenez-Munoz et al., 2014). That's why we used band 10 of Landsat 8 TIRS for LST retrieval for year 2018 of the study area and band 6 of Landsat 5 for the year 2001 and 2011 respectively.

For LST retrieval, atmospheric and radiometric correction are required which is applied to convert the digital number (DN) of thermal band data into top of atmosphere spectral radiance. The equation to convert DN values of thermal band to spectral radiance (Qin et al. 2001) is:

$$L_{(\lambda)} = L_{\min(\lambda)} + (L_{\max(\lambda)} - L_{\min(\lambda)})Q_{dn} / Q_{\max} \quad \text{.....(1)}$$

Where, $L_{(\lambda)}$ is the spectral radiance ($mW.cm^{-2}.sr^{-1}.\mu m^{-1}$), Q_{max} is the maximum DN value 255. Q_{dn} is the grayscale level for the analyzed pixel of the TM image, and $L_{min(\lambda)}$ and $L_{max(\lambda)}$ are the minimum and maximum detected spectral radiances for Q_{dn} = 0 and Q_{dn} =255 respectively.

The spectral radiance $L_{(\lambda)}$ of each thermal band for the three different year to at-satellite brightness temperature T_B conversion under the assumption of uni-form emissivity was done using the following formula:

$$T_B = \frac{K_2}{\ln(\frac{K_1}{L_\lambda}+1)} \quad \text{.....(2)}$$

Where, T_B is effective at-satellite temperature in degree kelvin, $L_{(\lambda)}$ is the spectral radiance and K_1 and K_2 are pre-launch calibration constants which is shown in table 2.

Table.2-Thermal Conversion Constants for Landsat

Constant	Landsat 5 (band 6)	Landsat 8 (band 10)
K_1 ($w/m^2/sr/\mu m$)	607.76	774.89
K_2 (degree Kelvin)	1260.56	1231.08

Source: (Fabeku et al., 2018)

The temperature values obtained above using Equation (2) are referenced to a blackbody. There is need for spectral emissivity corrections. Several studies used Normalized Difference Vegetation Index (NDVI) for the estimation of land surface emissivity (Sobrino, et al. 2004a) whereas other used land cover classification. But to avoid effect of classification error of land cover on land surface temperature, we used NDVI to estimate land surface emissivity. The equation to calculate NDVI is:

$$NDVI = \frac{NIR - RED}{NIR + RED} \quad \text{.....(3)}$$

Where, NIR=near-infrared and R=red band of Landsat data. The proportion of vegetation in each pixel was estimated using the following equation:

$$f_v = [\frac{NDVI - NDVI_s}{NDVI_v - NDVI_s}]^2 \quad \text{.....(4)}$$

Where, f_v is the proportion of vegetation in each pixel. $NDVI_s$ and $NDVI_v$ is the normalized difference vegetation index thresholds value for soil pixels ($NDVI_s$ =0.2) and pixels of full vegetation ($NDVI_v$=0.5) respectively (Sobrino et al. 1990)..

The cavity effect due to surface roughness computed suing the following equation:

$$C_\lambda = (1-\varepsilon_{s\lambda}) \times \varepsilon_{v\lambda} \times F \times (1-f_v) \quad \text{.....(5)}$$

Where, C_λ is the cavity effect and F is the geometrical (shape) factor with the mean value of 0.55 (Sobrino, et al. 1990).

The emissivity of a heterogeneous surface was computed using the following equation:

$$\varepsilon = \varepsilon_{v\lambda} \times f_v + \varepsilon_{s\lambda} \times (1-f_v) + C_\lambda \quad \text{.....(6)}$$

Where, ε_s and ε_v are the emissivity (ε) of soil pixels and full vegetation pixels with the mean value of 0.97 and 0.99 respectively (Sobrino, et al. 2004b).

Finally, the land surface temperature (S_{temp}) in degree Celsius was calculated as follows (Artis & Carnahan, 1982):

$$S_{temp} = \frac{T_B}{1+(\lambda \times T_B/\rho) \times \ln \varepsilon} - 273.15 \quad \text{.....(7)}$$

Where, T_B is effective at-satellite temperature in degree Kelvin (eq. 3), λ = wavelength of emitted radiance, $\rho = h \times c / \sigma$ = 1.48×10^{-2}m.K, h=Planck's constant (6.626×10^{-34} Js,c=velocity of light (2.998×10^{8} m/s) and σ =Boltzmann constant (1.38×10^{-23} J/K and ε =emissivity of surface.

By following all the mentioned steps and operations in Erdas Imagine software, the final land surface temperature maps were produced.

Land cover change & Land surface temperature: After preparing all the three land surface temperature maps and three land cover maps, the change detection of land cover over the years performed by using MOLUSCE plugin of QGIS software and the temperature was calculated by raster calculator. Land cover change detection was performed for the three years and analyzed the change throughout the time with temperature variation. As the urban area expand over the years, the urban heat island effect was also visible in temperature in every land cover classes.

3.Result & Discussion

Land cover classification & accuracy assessment:

For accuracy assessment, 200 random points generated in the classified map of year 2001, 2011 and 2018 respectively. Then the LULC class value of those points compared with Google Earth Historical Imagery for ground truth. Cohen kappa score for the classified(KNN) image of 2001 was 93%. This figure was 95% and 94% respectively for the year 2011 and 2018 which is better than other two algorithms (Table 3). Pontius (2002) and Sousa et al. (2002) suggested that kappa score greater than 0.8 represent excellent agreements between model and observed dataset. Accordingly, the classified LULC map by KNN show excellent agreement with observed LULC that's why the maps was used in further analysis.

Table.3- ***Accuracy assessment in different classifier***

Classification Algorithms	Kappa score		
	2001	2011	2018
Suport Vector Machine (SVM)	89%	88%	90%
Maximum likelihood	87%	90%	88%
K-nearest neighborhood (KNN)	93%	95%	94%

Land cover area calculation: Land cover area was calculated for the three years according to the class. According to the change map from 2001 to 2011, built up area was increased by 24.15%, vegetation was increased by 0.83% whereas, barren land was decreased by 23.65% and waterbody was decreased by 1.32%. According to the change map from 2011 to 2018, built up area was increased by 9.79% and water body by 0.81% whereas vegetation was decreased by 9.26% and barren land by 1.34%. So, it can be said that over the years, built up area had increased significantly whereas barren land and vegetation decreased.

Figure.1- ***Land cover classification for 2018,2011,2001***

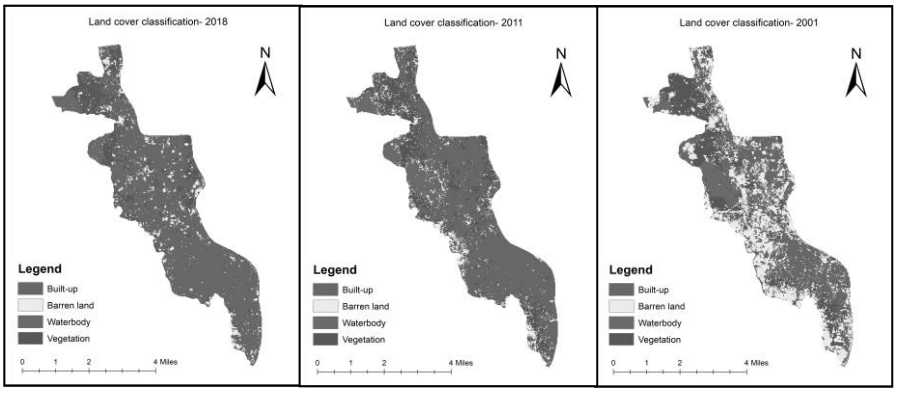

Table.4- ***Land cover area calculation for 2001,2011,2018***

Class / Area in Sq.km	2001	2011	2018
Built-up	15.06	25.92	30.34
Barren land	14.45	3.8	3.18
Waterbody	5.65	5.04	5.41
Vegetation	9.83	10.22	6.06

Land cover change detection: Land cover change detection was performed in QGIS to understand and analyze the area change among the classes over the years. Figure-2 shows the change detection map for 2001 to 2011 & 2011 to 2018.

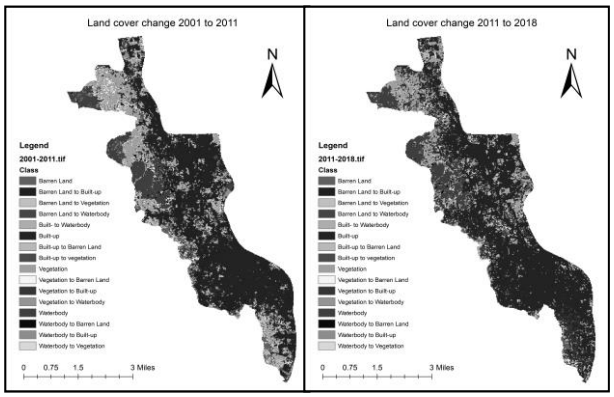

Figure.2- ***Land cover change map 2001-2011 & 2011-2018***

According to figure-2 of the change detection calculation for 2001 to 2011, the major change occurred in barren land to built-up area approximately converted 9.02 km^2, whereas barren land to vegetation was 2.46 $km^{2,}$, and vegetation to built-up was 2.24 km^2. So, it indicates that different class had transformed to built-up area in ten years. On the other hand, the change from 2011 to 2018 shows that, the major change occurred in vegetation to built-up area. Approximately 4.78 km^2 area converted. The conversion of barren land to built-up area was 1.54 $km^{2.}$. So, it indicates that, between 2011 and 2018-year, mainly vegetation land converted to built-up area.

Figure.3- ***Land surface temperature for 2001,2011,2018***

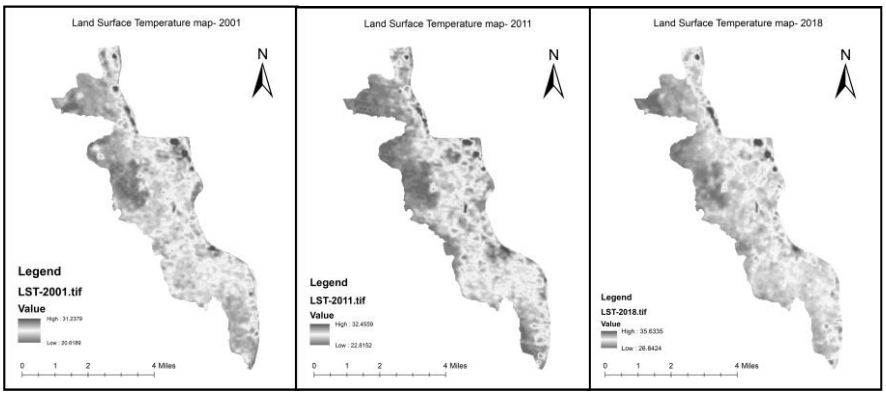

Urban heat island effect: Land surface temperature maps of the KCC area of three years represent the variation of the temperature spatially where dark red color represent the high temperature and blue color represent the low temperature in figure 3. It can be also said from the figure that, the average temperature is increased over time period as the average temperature in 2001 was 25.7^0 C where in 2011 was 27.6^0 C and in 2018 was 31.23^0 C. The minimum temperature was 20.61^0 C and maximum was 31.23^0 C in 2001, whereas in 2011, minimum was 22.81 and maximum was 32.45; in 2018 it was 26.81^0 C as minimum and 35.63^0 C as max temperature. So according to the LST analysis the temperature has increased by 5.5^0 C in last 17 years.

Urban heat island effect & Land cover change:

Table.4- Land cover class & LST

Class/LST(^{0}C)	2001			2011			2018		
	Avg.	Min	Max	Avg.	min	max	Avg.	Min	Max
Built-up	24.7	21.9	31.2	26.3	22.8	32.5	29.6	27.1	35.6
Barren land	24.0	21.1	30.4	24.4	22.8	27.1	29.5	27.4	32.7
Waterbody	22.0	20.6	25.8	23.8	22.8	27.9	28.1	26.8	33.0
Vegetation	23.0	21.1	26.7	24.6	22.8	28.4	28.7	27.1	34.7

Table.4 shows the temperature variation over the years according to land cover class. The analysis shows that the temperature of built-up area and barren land has increased significantly. From 2001 to 2018, The LST has increased in built-up area by 19.83%.

that temperature has increased in all the classes. So, as the land cover changes more to built-up area from 2001 to 2018, the LST has also increased proportionately. So the land cover change is directly co-related to the increasing temperature. As the study area getting more urbanized, more the temperature increase over the time in local climate. So it can be said that, the KCC area is also experiencing the urban heat island effect according to the land cover & LST analysis with the relationship considering the time duration from 2001 to 2018.

4.Conclusion: This study reveals the urban heat island effect on the study area by considering LST & Land cover change using GIS & remote sensing as integrated way in every spatial analysis and visualization. It is clear that LST has increased over the time when the land cover has also changed towards the more urban settings where built-up was increasing.so it is clear indication that as the area was getting more urban, the LST was also increasing in every land cover class which means relevant authority should take very effective and efficient planning interventions to mitigate this effect as soon as possible by controlling land cover change. This research can provide the guideline to identify the most vulnerable areas according to the rapid & drastic change of land cover along with the LST and necessary step can be taken through it.

5.Acknowledgement: The authors would like to thank Dr. Kazi saiful islam for his tremendous support to conduct this research and also grateful to USGS & Khulna City Corporation for the satellite data and boundary data.

6.References:

- Igun E, Williams M (2018) Impact of urban land cover change on land surface temperature. Global Journal of Environmental Science and Management 4: 47-58.
- Coskun HG, Alganci U, Usta G (2008) Analysis of land use change and urbanization in the Kucukcekmece water basin (Istanbul, Turkey) with temporal satellite data using remote sensing and GIS. Sensors 8: 7213-7223
- Becker, F. and Li, Z. (1990) Towards a Local Split Window Method over Land Surface. International Journal of Remote Sensing, 3, 17-33
- Sousa, S., Caciro, S., and Painho, M., 2002. Assessment of map similarity of categorical maps using Kappa statistics: The case of Sado estuary. ISEGI, Lisbon. Retrived from- https://unl-pt.academia.edu/MarcoPainho
- Pontius, R.G., 2002. Statistical methods to partition effects of quantity and location during comparison of categorical maps at multiple resolutions. Photogrammetric Engineering and Remote Sensing 68, 1041-1049.doi: 0099-1112/02/68lO-1041$3.00/0
- Sobrino, J., Jiménez-Muñoz, J., & Paolini, L. (2004a). Land surface temperature retrieval from LANDSAT TM 5. Remote Sensing Of Environment, 90(4), 434-440. doi: 10.1016/j.rse.2004.02.003
- Jimenez-Munoz, J., Sobrino, J., Skokovic, D., Mattar, C., & Cristobal, J. (2014). Land Surface Temperature Retrieval Methods From Landsat-8 Thermal Infrared Sensor Data. IEEE Geoscience And Remote Sensing Letters, 11(10), 1840-1843. doi: 10.1109/lgrs.2014.2312032
- Qin, Z., Karnieli, A., & Berliner, P. (2001). A mono-window algorithm for retrieving land surface temperature from Landsat TM data and its application to the Israel-Egypt border region. International Journal Of Remote Sensing, 22(18), 3719-3746. doi: 10.1080/01431160010006971
- Sobrino, J., Caselles, V., & Becker, F. (1990). Significance of the remotely sensed thermal infrared measurements obtained over a citrus orchard. *ISPRS Journal Of Photogrammetry And Remote Sensing*, *44*(6), 343-354. doi: 10.1016/0924-2716(90)90077-o
- Fabeku, B., Balogun, I., Adegboyega, S., & Faleyimu, O. (2018). Spatio-Temporal Variability in Land Surface Temperature and Its Relationship with Vegetation Types over Ibadan, South-Western Nigeria. Atmospheric And Climate Sciences, 08(03), 318-336. doi: 10.4236/acs.2018.83021
- Sobrino, J., Jiménez-Muñoz, J., El-Kharraz, J., Gómez, M., Romaguera, M., & Sòria, G. (2004b). Single-channel and two-channel methods for land surface temperature retrieval from DAIS data and its application to the Barrax site. International Journal Of Remote Sensing, 25(1), 215-230. doi: 10.1080/0143116031000115210
- Artis, D., & Carnahan, W. (1982). Survey of emissivity variability in thermography of urban areas. Remote Sensing Of Environment, 12(4), 313-329. doi: 10.1016/0034-4257(82)90043-8